WIS98/22/Aug. – DPP (quant-ph/9808058)

arXiv:quant-ph/9808058v2 12 Mar 1999

Dephasing and collapse in continuous measurement of a single system

S.A. Gurvitz

Department of Particle Physics, Weizmann Institute of Science, Rehovot 76100, Israel

(February 1, 2008)

Abstract

We show that long standing debates on the collapse and the role of the observer in quantum mechanics can be resolved experimentally via a nondistructive continuous monitoring of a single quantum system. An example of such a system, coupled with the point-contact detector is presented. The detailed quantum mechanical analysis of the entire system (including the detector) shows that under certain conditions the measurement collapse would generate distinctive effects in the detector behavior, which can be experimentally investigated.

I. INTRODUCTION

According to the principles of quantum mechanics, a system in the linear superposition of different states collapses to one of the states after the measurement. This is the wave-function collapse [1], which has been debated since the early days of quantum mechanics. The main question is of whether the collapse is originated by the interaction with detector. More precisely, is it described by the Schrödinger equation, $i\dot{\rho} = [\mathcal{H}, \rho]$, applied to the entire system. Here $\rho(\mathcal{S}, \mathcal{S}'; \mathcal{D}, \mathcal{D}', t)$ is the total density-matrix, where $\mathcal{S}(\mathcal{S}')$ and $\mathcal{D}(\mathcal{D}')$

are the variables of the measured system and the detector respectively, and $\mathcal{H}$ is the total Hamiltonian.

In order to determine of how the detector affects the measured system one needs to "trace out" the detector variables in the total density matrix,

$$\sum_D \rho(\mathcal{S}, \mathcal{S}', \mathcal{D}, \mathcal{D}, t) \to \sigma(\mathcal{S}, \mathcal{S}', t). \tag{1}$$

Since the detector is a macroscopic system, its density of states is very high (continuum). In this case the tracing generates an exponential damping of the off-diagonal terms ($\mathcal{S} \neq \mathcal{S}'$) ("decoherence"). As a result the reduced density-matrix of the observed system becomes the statistical mixture during the measurement, $\sigma(\mathcal{S}, \mathcal{S}', t) \to \bar{\sigma}(\mathcal{S}, \mathcal{S}', t)\delta_{\mathcal{S},\mathcal{S}'}$. The latter tells us that the system is actually in one of its states with the corresponding probability $\bar{\sigma}(\mathcal{S}, \mathcal{S}, t)$. Notice that such a tracing can be performed at any time t with no distortion of the Schrd̈inger equation of motion for the *entire* system, $i\dot{\rho} = [\mathcal{H}, \rho]$ [2,3]. Therefore the unitary evolution of the *entire* system is not violated.

Intensive investigations during last years demonstrated that in many cases the collapse can be attributed to the decoherence only [4]. Nevertheless, the real problem appears in a description of continuous nondistructive measurement of a *single* quantum object. Consider, for example, an electron oscillating between two different states (a and b) that are continuously monitored. We assume that these states are correlated with the macroscopically distinctive states A and B of the detector. As a result of interaction with the macroscopic detector, the electron oscillations are damped, so its reduced density-matrix approaches the statistical mixture, Eq. (1). In this limit the detector displays one of the states A or B. It tells us that the electron is found in one of the states, respectively, a or b. Then due to the measurement collapse the electron reduced density-matrix becomes a pure state $\sigma(\mathcal{S}, \mathcal{S}', t) \to \delta_{\mathcal{S},a}\delta_{\mathcal{S}',a}$ (the detector displays the state A). In this case the electron starts to oscillate again until the next quantum jump takes a place [5] etc.

It is rather clear that these quantum jumps cannot be attributed to the decoherence only. Moreover, their appearance is directly related to the wave function collapse. This

makes the study of a single quantum system under constant monitoring especially important for understanding of the measurement problems [6]. In addition, such a study have even practical applications. This is in view of a possible use of single quantum systems for quantum computing [7].

An essential point, which is missed in many studies of quantum measurements is a detailed quantum mechanical treatment of the entire system, that is, of the detector and the measured system together [8]. The reason is that the detector is a macroscopic device, the quantum mechanical analysis of which is rather complicated. Thus one can expect that the mesoscopic systems, which are between the microscopic and macroscopic scales, would be very useful for this type of investigation [9]. A generic example of such a system has been considered in [3]. It consisted of two coupled quantum dots, occupied by one electron, and the point-contact detector [10], monitoring the occupation of one of the dots [11]. The system has been analyzed by using the Bloch-type rate equations for the density-matrix, obtained directly from the many-body Schrödinger equation [2,3]. These equations describe the behavior of both, the observed electron and the macroscopic (mesoscopic) detector, in the most transparent and simple way.

In this paper we perform such a "simultaneous" microscopic study of the detector and the measured system during the continuous measurement for the setup proposed in [3,6]. This analysis would explicitly show where the problem of the wave function collapse emerges and in what way it affects the experimental outcome. Therefore it may open a possibility for experimental investigation of the measurement problem.

The plan of the paper is as follows: In Sect. 2 we describe the Bloch-type rate equation for the entire system and their quantum-mechanical microscopic origin. In Sect. 3 we discusses the microscopic behavior of the detector, separated from the measured system. In Sect. 4 we concentrate on the quantum mechanical behavior of the detector during the measurement process. The necessity for the measurement collapse, is explained. We discuss its different scenarios and their experimental consequences. The last section is Discussion. The details of quantum mechanical derivation of the classical rate equations for the point-

contact detector are given in Appendix, as well as the evaluation of the average current and the current fluctuation.

II. CONTINUOUS MONITORING OF A SINGLE ELECTRON WITH THE POINT-CONTACT DETECTOR

A. General description

Consider the measurement of a single electron oscillating in the double-dot by using the point-contact detector [10,11]. Such a set up is shown schematically in Fig. 1, where

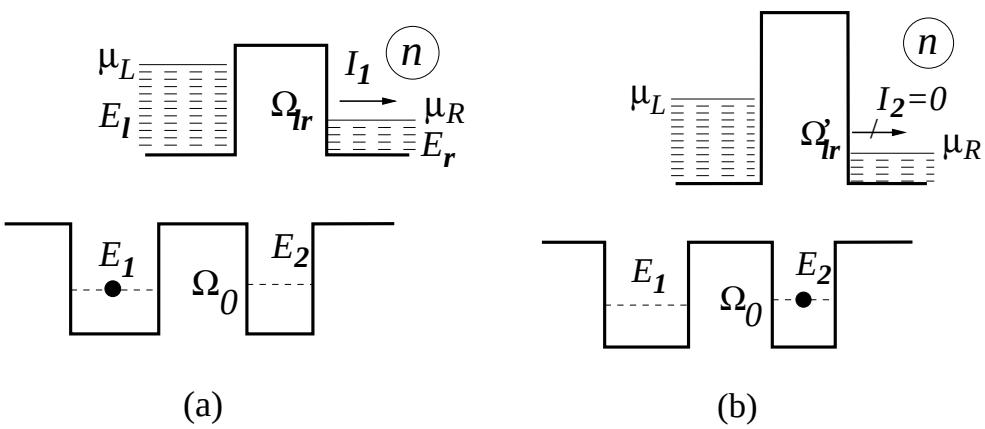

Fig. 1. The point-contact detector near the double-dot. Ω_{lr} is the coupling between the level E_l and E_r in the left and the right reservoirs. Ω_0 is the coupling between the quantum dots. The index n denotes the number of electrons penetrating to the right reservoir (collector) at time t.

the point-contact, represented by the barrier, is placed near one of the dots. The barrier is connected with two reservoirs at the chemical potentials μ_L and $\mu_R = \mu_L - V_d$ respectively, where V_d is the applied voltage. Since $\mu_L > \mu_R$, the current $I = eTV_d/(2\pi)$ flows through the point-contact [12], where e is the electron charge and T is the transmission coefficient of the point-contact. (We choose the units where $\hbar = 1$). The penetrability of the point-contact (the barrier height) is modulated by the electron, oscillating inside the double-dot. When

the electron occupies the left dot, the transmission coefficient is T_1. However, when the right dot is occupied, the transmission coefficient $T_2 \ll T_1$ due to the electrostatic repulsion generated by the electron. As a result, the current $I_2 \ll I_1$. Without loosing generality we assume that $T_2 = 0$, so that the point contact is blocked whenever the right dot is occupied. Since the difference $\Delta I = I_1 - I_2$ is macroscopically large, one can determine which of the dots is occupied by observing the point-contact current. Yet, the entire system can be treated quantum-mechanically. For its description we use the following tunneling Hamiltonian [3]:

$$\mathcal{H} = \mathcal{H}_{PC} + \mathcal{H}_{DD} + \mathcal{H}_{int}, \tag{2}$$

where

$$\mathcal{H}_{PC} = \sum_l E_l a_l^\dagger a_l + \sum_r E_r a_r^\dagger a_r + \sum_{l,r} \Omega_{lr}(a_l^\dagger a_r + a_r^\dagger a_l)\,, \tag{3a}$$

$$\mathcal{H}_{DD} = E_1 c_1^\dagger c_1 + E_2 c_2^\dagger c_2 + \Omega_0(c_2^\dagger c_1 + c_1^\dagger c_2)\,, \tag{3b}$$

$$\mathcal{H}_{int} = -\sum_{l,r} \Omega_{lr} c_2^\dagger c_2 (a_l^\dagger a_r + a_r^\dagger a_l)\,. \tag{3c}$$

Here $\mathcal{H}_{PC}$, $\mathcal{H}_{DD}$ and $\mathcal{H}_{int}$ are the Hamiltonians describing the point-contact, double-dot and their mutual interaction, respectively, $E_{l,r}$ are the energy levels in the left (right) reservoir, and Ω_{lr} is the coupling between the reservoirs. It is related to the penetration coefficient by $(2\pi)^2\Omega^2\rho_L\rho_R = T$, where $\rho_{L,R}$ are the density of states in the left (right) reservoir [13]. If the left well is occupied, the coupling $\Omega'_{lr} = 0$ due to the interaction term, $\mathcal{H}_{int}$. In fact, the Hamiltonian $\mathcal{H}$ should include additional terms for a macroscopic device that actually counts the charge transmitted to the detector (the pointer). This question is considered later in a more detail. In any case such a pointer would not affect the (macroscopic) detector current [14], and therefore the observed electron. It implies that we can consider the measurement setup shown in Fig. 1 as the *closed* system, describing by the Hamiltonian (2).

For simplicity we consider the reservoirs at zero temperature and the entire system in a pure state, i.e. we describe it by the wave-function. The latter can be written as

$$|\Psi(t)\rangle = \exp(-i\mathcal{H}t)|0\rangle = \Bigg[b_1(t)c_1^\dagger + \sum_{l,r} b_{1lr}(t) c_1^\dagger a_r^\dagger a_l + \sum_{l<l',r<r'} b_{1ll'rr'}(t) c_1^\dagger a_r^\dagger a_{r'}^\dagger a_l a_{l'}$$

$$+ \; b_2(t)c_2^\dagger + \sum_{l,r} b_{2lr}(t)c_2^\dagger a_r^\dagger a_l + \sum_{l<l',r<r'} b_{2ll'rr'}(t)c_2^\dagger a_r^\dagger a_{r'}^\dagger a_l a_{l'} + \cdots \Bigg] |0\rangle, \tag{4}$$

where $b(t)$ are the probability amplitudes to find the system in the states defined by the corresponding creation and annihilation operators. The "vacuum" state $|0\rangle$ corresponds to the left and the right reservoirs (the emitter and the collector) are filled up to the Fermi levels μ_L and μ_R, respectively.

Substituting Eq. (4) into the Shrödinger equation $i|\dot{\Psi}(t)\rangle = \mathcal{H}|\Psi(t)\rangle$ we find an infinite set of equations for the amplitudes $b(t)$. Then, performing summation (integration) over the reservoir states $(l, l', \ldots, r.r', \ldots)$, we can transform the Shrödinger equation for the amplitudes $b(t)$ into differential equations for the reduced density-matrix $\sigma_{i,j}^{(n)}(t)$ of the entire system, where

$$\sigma_{ij}^{(0)}(t) = b_i(t)b_j^*(t), \qquad \sigma_{ij}^{(1)}(t) = \sum_{l,r} b_{ilr}(t)b_{jlr}^*(t), \qquad \sigma_{ij}^{(2)}(t) = \sum_{ll',rr'} b_{ill'rr'}(t)b_{jll'rr'}^*(t), \; \cdots \tag{5}$$

and $i, j = \{1, 2\}$ denote the occupied states of the double-dot system. The index n denotes the number of electrons, penetrating to the right reservoir at time t. Detailed microscopic derivation of these equations for quantum transport can be found in [3,2], and in the Appendix. Here we present only the final result for our system [3]:

$$\dot{\sigma}_{11}^{(n)} = -D_1\sigma_{11}^{(n)} + D_1\sigma_{11}^{(n-1)} + i\Omega_0(\sigma_{12}^{(n)} - \sigma_{21}^{(n)}) \; , \tag{6a}$$

$$\dot{\sigma}_{22}^{(n)} = -i\Omega_0(\sigma_{12}^{(n)} - \sigma_{21}^{(n)}) \; , \tag{6b}$$

$$\dot{\sigma}_{12}^{(n)} = i\epsilon\sigma_{12}^{(n)} + i\Omega_0(\sigma_{11}^{(n)} - \sigma_{22}^{(n)}) - \frac{D_1}{2}\sigma_{12}^{(n)} \; , \tag{6c}$$

where $\epsilon = E_2 - E_1$, and $D_1 = T_1V_d/(2\pi)$, Fig. 1. These equations have clear physical interpretation. Consider, for instance, Eq. (6a) for the probability rate of finding the system in the state, shown in Fig. 1a. The latter decays to the state with $(n+1)$ electrons in the collector with the rate D_1. This process is described by the first term in Eq. (6a). On the other hand, there exists the opposite ("gain") process (with the same rate D_1), when the state with $(n-1)$ in the collector converts to the state with n electrons in the collector. It is described by the second term in Eq. (6a). All these processes are generated by one-electron transitions between continuum states. If, however, one-electron transition takes

place between *isolated* states, it results in a coupling between diagonal and off-diagonal density-matrix elements (in our case it is given by the last term in Eq. (6a)).

The evolution of the off-diagonal density-matrix elements $\sigma_{12}^{(n)}$ is given by Eq. (6c). It can be interpret in the same way as the rate equations for the diagonal terms. Notice, however, the absence of the gain term in Eq. (6c). Such a term would be generated by one-electron hopping ($n-1 \to n$), resulting in $\sigma_{12}^{(n-1)} \to \sigma_{12}^{(n)}$ transition. Yet, in our case this transition is not possible, since the point-contact is blocked when the right dot is occupied, Fig. 1b.

Eqs. (6) look as the Bloch-type optical rate equations. Yet, Eqs. (6) were obtained from the many-body Schrödinger equation for the entire system. No stochastic assumptions have made in their derivation, despite the master-equations structure of Eqs. (6). In addition, these equations describe quantum transport on the microscopic level, in contrast with the usual master-equation, holding only on a coarse-grained time scale.

B. Time-evolution of the measured system in the presence of detector

Although Eqs. (6) have a rather simple form, they describe the microscopic behavior of the measured system and the detector at once. In order to find the time-evolution of the measured system we trace out the detector states n, thus obtaining

$$\dot{\sigma}_{11} = i\Omega_0(\sigma_{12} - \sigma_{21}) \ , \tag{7a}$$

$$\dot{\sigma}_{22} = i\Omega_0(\sigma_{21} - \sigma_{12}) \ , \tag{7b}$$

$$\dot{\sigma}_{12} = i\epsilon\sigma_{12} + i\Omega_0(\sigma_{11} - \sigma_{22}) - \frac{1}{2}\Gamma_d\sigma_{12}. \tag{7c}$$

where $\sigma_{ij} = \sum_n \sigma_{ij}^{(n)}$, and $\Gamma_d = D_1$ is the dephasing rate generated by the detector.

As expected, the asymptotic solution of Eqs. (7) is always the statistical mixture:

$$\sigma(t) = \begin{pmatrix} \sigma_{11}(t) & \sigma_{12}(t) \\ \sigma_{21}(t) & \sigma_{22}(t) \end{pmatrix} \stackrel{t\to\infty}{\longrightarrow} \begin{pmatrix} 1/2 & 0 \\ 0 & 1/2 \end{pmatrix}. \tag{8}$$

Yet, the relevant relaxation time depends on the initial conditions. Consider for instance the initial conditions $\sigma_{11}(0) = 1$, $\sigma_{22}(0) = \sigma_{12}(0) = 0$ corresponding to the electron localized

in the left dot. Solving Eqs. (7) for the aligned levels ($\epsilon = 0$) we find

$$\sigma_{11}(t) = \frac{1}{2} + \frac{1}{4}\left(1 + \frac{\Gamma_d}{\omega}\right) e^{-e_- t} + \frac{1}{4}\left(1 - \frac{\Gamma_d}{\omega}\right) e^{-e_+ t} \tag{9a}$$

$$\sigma_{12}(t) = i\frac{4\Omega_0}{\omega}\left(e^{-e_- t} - e^{-e_+ t}\right) , \tag{9b}$$

where $\omega = \sqrt{\Gamma_d^2 - 64\Omega_0^2}$, and $e_\pm = \frac{1}{4}(\Gamma_d \pm \omega)$. Therefore $e_+ \simeq \Gamma_d/2$ and $e_- \simeq 8\Omega_0^2/\Gamma_d$ in the limit of $\Gamma_d \gg 8\Omega_0$. As a result the relaxation time (τ_Z) *increases* with Γ_d:

$$\tau_Z = \frac{4}{\Gamma_d - \mathrm{Re}\ \omega} \to \frac{\Gamma_d}{8\Omega_0^2}, \quad \text{for} \quad \Gamma_d \gg 8\Omega_0 \,. \tag{10}$$

Hence, the electron stays in the left dot for a long time, Fig. 2a, which is the quantum Zeno effect [15]. We therefore called this relaxation time as the "Zeno" time, τ_Z. Notice an emergence of the off-diagonal density-matrix term, $\sigma_{12}(t)$, that actually govern the electron transition between the dots during the relaxation period ($t < \tau_Z$).

If however, the electron is initially in the ground state (the symmetric superposition), the relaxation time is much shorter ($\tau_Z \sim \Gamma_d^{-1}$), Fig. 2b. Indeed, in this case one obtains from Eq. (7) that $\sigma_{11}(t) = \sigma_{22}(t) = 1/2$ and $\sigma_{12}(t) = (1/2)\exp(-\Gamma_d t/2)$.

We thus obtained that the probability of finding the electron in the first dot is given by $\sigma_{11}(t)$, Eqs. (7). Consider now the point-contact current I. Since it is monitored by occupation of the first dot, Fig. 1, one could expect that $I(t) = I_1\sigma_{11}(t)$. In fact, the same result is obtained by evaluating of $\langle I(t)\rangle = \langle\Psi(t)|\hat{I}|\Psi(t)\rangle$, where $\hat{I} = i\,[\mathcal{H}, Q_R]$ and $Q_R = e\sum_r a_r^\dagger a_r$ is the charge accumulated in the right reservoir [3]. This, however, would imply that the detector displays the current $I_1/2$, whenever the electrons density-matrix becomes the mixture, Eq. (8). On the other hand, the mixture means that the electron actually occupies one of the dots. As a result, the detector should show either I_1 or 0, but not $I_1/2$. As a matter of fact the both statements are not in a contradiction, since $\langle I(t)\rangle$ represents the average detector current, but not its actual value. Thus, the time-dependence of the detector current is not always determined by the electron density-matrix $\sigma_{11}(t)$. Actually, this cannot be surprising, since the observable quantity is the number of electrons (n) arriving to the collector. The latter is given by the total density-matrix

$\sigma_{ij}^{(n)}$, Eqs. (6), which we are now going to evaluate. This would allow us to understand the detector behavior during the measurement process.

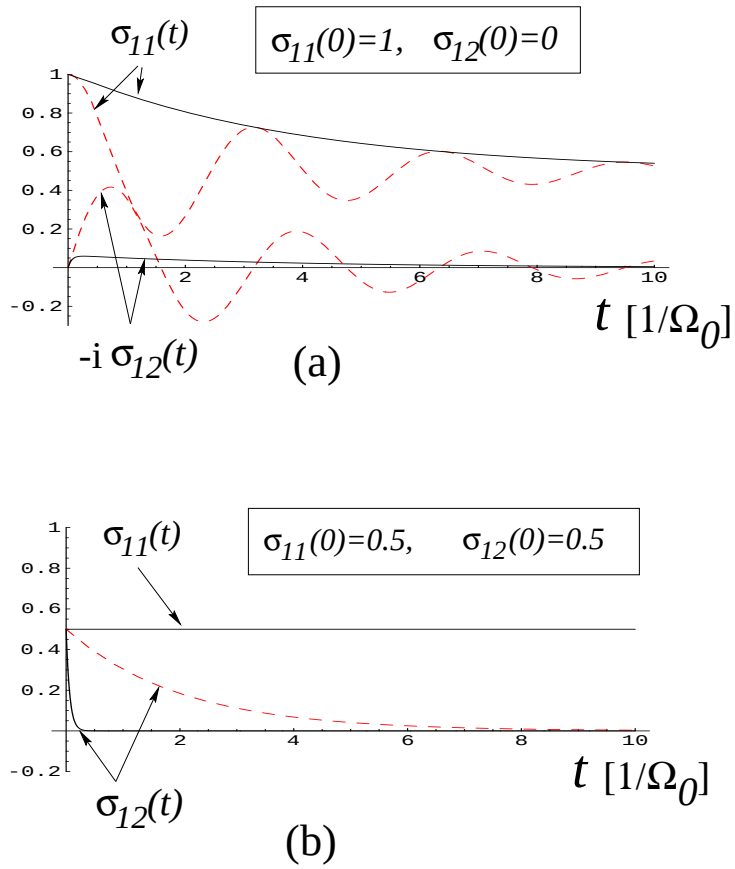

Fig. 2. The occupation probability of the first well (σ_{11}) and the nondiagonal density-matrix element (σ_{12}) as a function of time for $\epsilon = 0$, and two values of the dephasing rate: $\Gamma_d = \Omega_0$ (dashed lines), and $\Gamma_d = 32\Omega_0$ (solid lines). The initial conditions: (a) the electron occupies the first dot, (b) the electron is in the ground state.

III. MICROSCOPIC BEHAVIOR OF THE POINT-CONTACT DETECTOR

First we investigate the motion of carriers through the point-contact, decoupled from the double-dot. We thus put $\Omega_0 = 0$ in Eqs. (6), so that the electron stays in left dot all the time. In this case the detector is described by Eq. (6a), which now reads

$$\dot{p}_n(t) = -D_1 p_n(t) + D_1 p_{n-1}(t) \ , \tag{11}$$

where $p_n(t) \equiv \sigma_{11}^{(n)}(t)$ is the probability of finding n electrons in the collector at time t. The initial condition, $p_n(0) = \delta_{n0}$, corresponds to zero electrons in the collector.

Eq. (11) looks as a pure classical rate equation. Yet, no "classical" assumptions beyond quantum-mechanical treatment were made in its derivation [3]. Since this point is very important in the following discussion, we present in Appendix the quantum mechanical derivation of Eq. (11) and determine conditions for its validity.

Eq. (11) can be easily solved by applying the Fourier transform [16]: $\tilde{p}(k,t) = \sum_n p_n(t) \exp(ink)$. One finds

$$\tilde{p}(k,t) = \exp\left[-D_1(1-e^{ik})t\right] \ . \tag{12}$$

The distribution $p_n(t)$ is given by the inverse Fourier transform of $\tilde{p}(k,t)$. Using the stationary phase approximation we obtain

$$p_n(t) = \frac{1}{2\pi}\int_{-\pi}^{\pi} \tilde{p}(k,t)\exp(-ink)dk \simeq \frac{1}{\sqrt{2\pi D_1 t}} \exp\left[-\frac{(D_1 t - n)^2}{2D_1 t}\right] . \tag{13}$$

This implies that $p_n(t)$ can be viewed as a wave packet of the width $\sqrt{2D_1 t}$ propagating in the n-space with the group velocity D_1. Thus, the number of electrons accumulated in the collector is $< n(t) >= D_1 t$ that corresponds to the detector current $I = eD_1$. Notice that $< n(t) >$ can reach macroscopic values in a very short time, providing that D_1 is large enough. In the following we consider the number of electrons accumulated in the collector as the observed quantity (instead of the detector current). Note that the corresponding operator $\hat{N} = \sum_r a_r^\dagger a_r$ commutes with the operator $c_i^\dagger c_j$, so that the observation of n does not influence the double-dot electron.

IV. THE DETECTOR BEHAVIOR IN THE PRESENCE OF DOUBLE-DOT

Consider now $\Omega_0 \neq 0$. Let us evaluate the probability $P_n(t)$ of finding n electrons in the collector at time t. In order to obtain this quantity we trace the density-matrix over the states of the *measured system* (cf. with Eqs. (7)): $P_n(t) = \sigma_{11}^{(n)}(t) + \sigma_{22}^{(n)}(t)$, where $\sigma_{ii}^{(n)}$ are given by Eqs. (6). As in the previous case we apply the Fourier transform [16]: $\tilde{\sigma}_{ij}(k,t) = \sum_n \sigma_{ij}^{(n)}(t)\exp(ink)$. Then Eqs. (6) become:

$$\dot{\tilde{\sigma}}_{11} = -D_1(1-e^{ik})\tilde{\sigma}_{11} + 2i\Omega_0\Delta\tilde{\sigma}_{12} \ , \tag{14a}$$

$$\dot{\tilde{\sigma}}_{22} = -2i\Omega_0\Delta\tilde{\sigma}_{12} \ , \tag{14b}$$

$$\Delta\dot{\tilde{\sigma}}_{12} = i\Omega_0(\tilde{\sigma}_{11} - \tilde{\sigma}_{22}) - \frac{D_1}{2}\Delta\tilde{\sigma}_{12} \ , \tag{14c}$$

where $\Delta\tilde{\sigma}_{12} = (\tilde{\sigma}_{12} - \tilde{\sigma}_{21})/2$. For simplicity we considered here the case of aligned levels, $\epsilon = 0$. Note that $D_1 \equiv \Gamma_d$ is the decoherence rate in Eq. (7c). Next, by applying the Laplace transform, $s(k,E) = \int_0^\infty \tilde{\sigma}(k,t)\exp(iEt)dt$, we reduce Eqs. (14) to a system of linear algebraic equations:

$$\begin{pmatrix} E + iD_1(1-e^{ik}) & 0 & 2\Omega_0 \\ 0 & E & -2\Omega_0 \\ \Omega_0 & -\Omega_0 & E + iD_1/2 \end{pmatrix} \begin{pmatrix} s_{11} \\ s_{22} \\ \Delta s_{12} \end{pmatrix} = \begin{pmatrix} i\sigma_{11}^{(0)}(0) \\ i\sigma_{22}^{(0)}(0) \\ \mathrm{Im}\ \sigma_{21}^{(0)}(0) \end{pmatrix} \tag{15}$$

where the r.h.s. is defined by the initial condition.

Solving Eqs. (15) and performing the inverse Laplace and Fourier transformations we obtain

$$P_n(t) = \sum_{\substack{j=1 \\ (j'>j''\neq j)}}^{3} \int_{-\pi}^{\pi} \frac{dk}{2\pi} \frac{\mathcal{M}(e_j)}{(e_j - e_{j'})(e_j - e_{j''})} \exp(-ie_j t - ink) \, , \tag{16}$$

where $e_{1,2,3}$ are the roots of the secular determinant and $\mathcal{M}$ is the corresponding minor determinant. The secular determinant is represented by a cubic equation. We solve it perturbatively in the limits of weak and strong decoherence (damping).

A. Weak damping ($D_1 \ll \Omega_0$)

Consider for the definiteness the initial conditions $\sigma_{11}^{(0)}(0) = 1$ and $\sigma_{22}^{(0)}(0) = \sigma_{12}^{(0)}(0) = 0$, corresponding to the electron localized in the left dot, Then $\mathcal{M} = e_j(e_j + iD_1/2) - 4\Omega_0^2$ in Eq. (16). The roots of the secular equation in the case of weak damping are $e_1 \simeq -iD_1\xi/2$ and $e_{2,3} \simeq \pm 2\Omega_0$, where $\xi = 1 - \exp(ik)$. It is clear from Eq. (16) that the dominant contribution is coming from the first root. Using the stationary phase approximation we find the following expression for $P_n(t)$

$$P_n(t) = \frac{1}{\sqrt{\pi D_1 t}} \exp\left[-\frac{(D_1 t/2 - n)^2}{D_1 t}\right]. \tag{17}$$

It looks as Eq. (13) for the undistorted motion of carriers through the point-contact, except for the group velocity, $D_1/2$. The latter corresponds to the "average" value of the detector current ($I_1/2$). The interpretation of this result is very simple. Since $\Omega_0 \gg D_1$, the observed electron oscillates many times between the dots during the time of an electron penetration to the collector. As a result the detector current displays the average electron charge ($e/2$) in each of the dots.

In fact, the same average current $I_1/2$ would be displayed even for $D_1 \simeq \Omega_0$. This can be seen from Fig. 3 that shows $P_n(t)$, obtained from a numerical solution of Eqs. (6) for $D_1 = \Omega_0$ (bars), in a comparison with the distribution $p_n(t)$ (solid lines), obtained from Eq. (11) for $D_1 = \Omega_0/2$. It follows from this figure that the distribution of electrons arriving to the collector corresponds to the current $I_1/2$ flowing through the point-contact. This implies that the electron oscillations between the dots, shown in Fig. 2a by the dashed line would not be reflected in the behavior of the point-contact current. Therefore, the point-contact cannot be a good detector in the case of weak damping [17].

This example clearly demonstrates that the time-dependence of the detector current $I_d(t)$ is not fully determined by the density-matrix of the observed electron via the relation $I_d(t) = eD_1\sigma_{11}(t)$ [3]. The latter represents an ensemble average over the electron in the double-dot. In each particular experiment, however, the electron oscillation between the dots

cannot be seen. We believe that this is the reason of a disagreement with recent predictions for the detector current behavior for the case of weak damping [18,19].

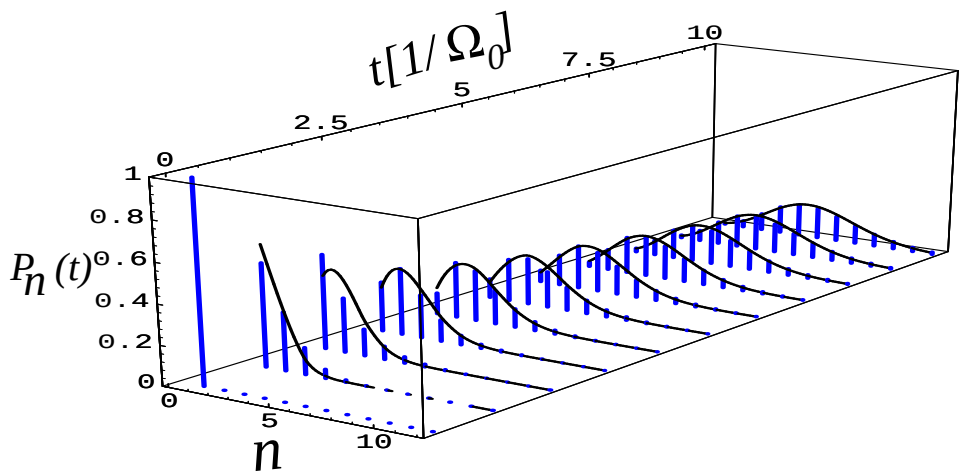

Fig. 3. Probability distribution of electrons in the collector, $P_n(t)$, for $D_1 = \Omega_0$. The electron is initially localized in the left dot. The solid lines represent smooth interpolation of $p_n(t)$, Eq. (11) for $D_1 = \Omega_0/2$.

B. Strong damping ($D_1 \gg \Omega_0$)

1. The electron is initially in the left dot

Consider now the strong decoherence limit, $D_1 \gg \Omega_0$. In this case many electrons can penetrate to the collector during one oscillation of the observed electron. Thus, the point-contact should represent a good detector in this case. However, the strong decoherence would result in quantum Zeno effect, which hinders the electron transitions between the dots. Let us investigate how this effect is reflected in the detector behavior.

Solving the secular equation perturbatively, we obtain the following expressions for the roots e_j, Eq. (16)

$$e_{1,2} = -i\left(\frac{D_1\xi}{2} + \frac{4\Omega_0^2}{D_1} \mp \sqrt{\frac{D_1^2\xi^2}{4} + \frac{16\Omega_0^4}{D_1^2}}\right) + \mathcal{O}\left[\frac{\Omega_0^2}{D_1}\right]^2 , \tag{18a}$$

$$e_3 = -i\frac{D_1}{2} + i\frac{8\Omega_0^2}{D_1}(1+\xi) + \mathcal{O}\left[\frac{\Omega_0^2}{D_1}\right]^2 . \tag{18b}$$

where $\xi = 1 - \exp(ik)$. The minor determinant $\mathcal{M}$ in Eq. (16) is the same as in the previous case. Substituting Eqs. (18) into Eq. (16) we find that the main contribution is coming from the roots $e_{1,2}$. The contribution from the third root is $\propto \exp(-D_1 t/2)$, and therefore it can be important only at very short times, $t < 2/D_1$.

Consider first the distribution $P_n(t)$ in the time-interval $2/D_1 \lesssim t \lesssim \tau_Z$, when the electron stays localized in the first dot (Fig. 2a). Then the main contribution to the integral (16) is coming from $k \simeq 1/n \gg 8\Omega_0^2/D_1^2$. In this region $e_1 \simeq -4i\Omega_0^2/D_1$ and $e_2 \simeq -iD_1\xi + e_1$, Eq. (18a). Substituting these values into Eq. (16) and neglecting the terms of higher orders in $\Omega_0^2/(D_1^2\xi)$ and ξ we find that $P_n(t) = p_n(t)$, Eq. (13). This means that the distribution $P_n(t)$ does indeed correspond to the electron localized in the left dot. Thus, the detector would display the current $I_1 = eD_1$ during the time-interval $t \lesssim \tau_Z$, in an agreement with the behavior of the reduced electron density-matrix, Eq. (9), Fig. 2a.

In order to confirm the validity of the above result we show in Fig. 4 the distribution of $P_n(t)$ (bars), obtained from the numerical solution of Eqs. (6) for $0 \leq t \leq \Omega_0^{-1}$ and $D_1 = 32\Omega_0$. For comparison we display the distribution $p_n(t)$, Eq. (11), corresponding to the current $I_1 = eD_1$ flowing through the contact. One finds that that in an agreement with our analytical calculations. the distributions $P_n(t)$ and p_n are practically indistinguishable.

Consider now the probability distribution $P_n(t)$ for $t \gg \tau_Z$, when the electron density matrix becomes the mixture, Eq. (8). It corresponds to $k \simeq 1/n \ll 8\Omega_0^2/D_1^2$ in Eq. (16). Using Eq. (18a) one finds that $e_1 \simeq -iD_1\xi/2$ and $e_2 \simeq -8i\Omega_0^2/D_1 + e_1$. This implies that the term $\propto \exp(-ie_2 t)$ in Eq. (16) is exponentially suppressed for $t \gg \tau_Z$. Eventually, it is only the term $\propto \exp(-ie_1 t)$ that survives in the "asymptotic" limit. As a result we arrive to Eq. (17) for $P_n(t)$ in the limit of $t \gg \tau_Z$. This represents the "average" detector current $(I_1/2)$. Actually, one can easily demonstrate that the "asymptotic" behavior of $P_n(t)$, given

by Eq. (17) is valid for any relation between D_1 and Ω_0, and for any initial conditions.

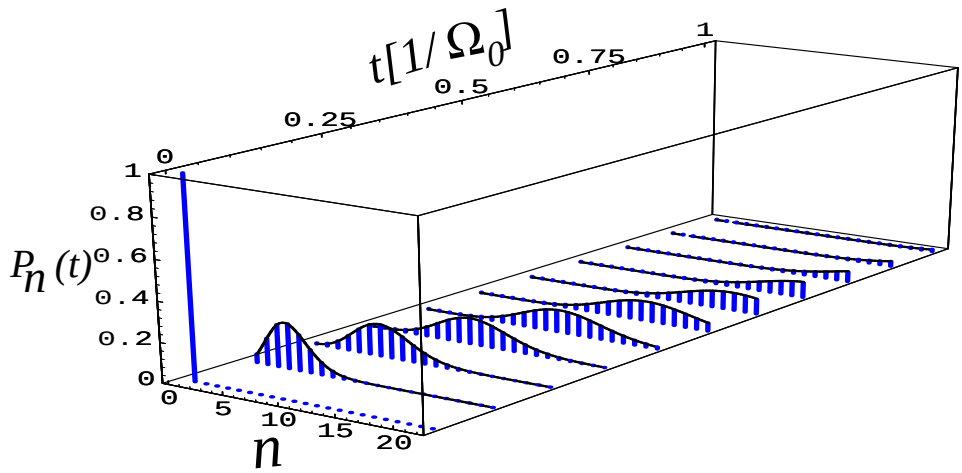

Fig. 4. Probability distribution of electrons in the collector, $P_n(t)$, for $t \leq \Omega_0^{-1}$ and $D_1 = 32\Omega_0$. The electron is initially localized in the left dot. The solid lines represent smooth interpolation of $p_n(t)$, Eq. (11), corresponding to the electron permanently localized in the left dot.

Thus, we found that in the case of strong damping and the electron is initially localized in one of the dots, the detector current behaves in an accordance with the electron density-matrix, $I_d(t) = eD_1\sigma_{11}(t)$. Indeed, the detector displays the current I_1 for $t \lesssim \tau_Z$, and the average current, $I_1/2$, for $t \gg \tau_Z$, i.e. when the electron density-matrix becomes the mixture.

2. The electron is initially in the ground state

Let us solve Eq. (15) for the initial conditions $\sigma_{11}^{(0)}(0) = \sigma_{22}^{(0)}(0) = \sigma_{12}^{(0)}(0) = \frac{1}{2}$, corresponding to the double-dot electron in the ground state. (Actually, the same result would be obtained if the electron is initially in the statistical mixture). Then

$$\mathcal{M} = e_j[2e_j + iD_1(1+\xi)] - \frac{1}{2}D_1^2\xi - 8\Omega_0^2 \tag{19}$$

in Eq. (16). If the detector behavior is determined by the electron density-matrix $\sigma_{ij}(t)$, than the distribution $P_n(t)$ should display the "average" current $I_1/2$, corresponding to Eq. (17), already for $t \gg 2/D_1$, when $\sigma_{ij}(t)$ becomes the the mixture, (Fig. 2b). Yet, it is not the case. One obtains from Eq. (16)

$$P_n(t) = \frac{1}{2}\delta_{n,0}\exp\left(-\frac{4\Omega_0^2}{D_1}t\right) + \frac{1}{2}p_n(t)\,, \tag{20}$$

where $p_n(t)$ is given by Eq. (13), and we neglected the terms of higher orders in $\Omega_0^2/(D_1^2\xi)$ and ξ. Thus we find that $P_n(t)$, given by Eq. (20), is very different from that given by Eq. (17), despite of the corresponding electron density matrix is almost the statistical mixture in the both cases.

In order to confirm our analytical calculations we present in Fig. 5 the distribution $P_n(t)$ (bars) as a function of n and t, found from the numerical solution of Eqs. (6) for $0 \le t \le \Omega_0^{-1}$ and $D_1 = 32\Omega_0$. The solid lines represent $\frac{1}{2}p_n(t)$ as given by Eq. (11). Thus, Eq. (20) represents the exact result quite well. It is also in a qualitative agreement with the recent numerical calculations [16].

It follows from Eq. (20) and Fig. 5 that $P_n(t)$ displays two peaks, at $n = 0$ and $n = D_1t$, which remain separated for a long time ($\sim \tau_Z$). This implies that one finds either zero or $n \simeq D_1t$ electrons with the probability 1/2 at any time $1/D_1 \lesssim t \lesssim \tau_Z$. If we assume that an actual observation of the accumulated charge (en) does not affect the evolution of $P_n(t)$, then the repeated observations would show unlimited fluctuations of electron charge in the collector (for $\tau_Z = D_1/8\Omega_0^2 \to \infty$). Such a scenario looks impossible. Hence, we have to assume that the "actual fact" happens at some time, so that one of these two possibilities is actually realized. At that moment the evolution of $P_n(t)$ starts with the new initial conditions. It looks as a quantum jump [5], which however, is not generated by quantum evolution of the entire system, Eqs. (6). Now we consider this problem in more details.

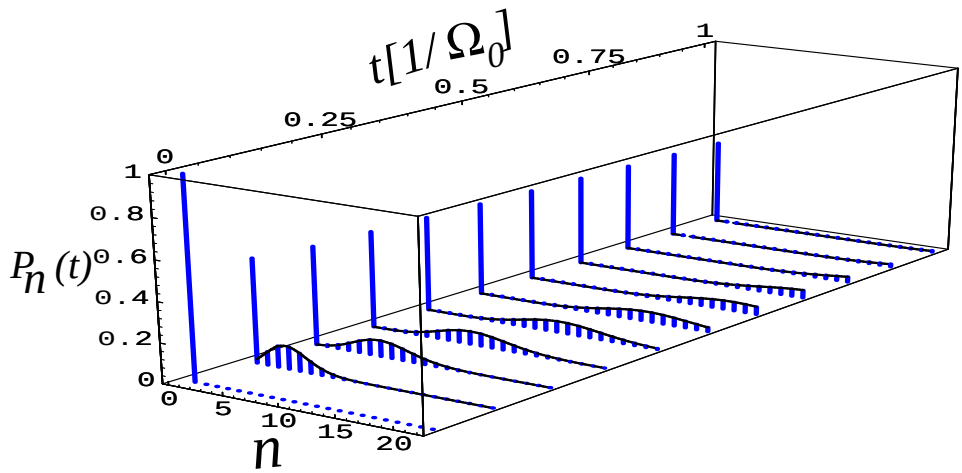

Fig. 5. Probability distribution of $P_n(t)$ for $t \leq \Omega_0^{-1}$ for the initial condition corresponding to the electron in the symmetric superposition, and $D_1 = 32\Omega_0$. The solid lines show the smooth interpolation of $\frac{1}{2}p_n(t)$, Eq. (11).

V. COLLAPSE AND THE ROLE OF OBSERVER

We demonstrated in the previous example that an uncertainty of finding the electron in one of the dots leads to the possibility of observing either zero or large number of electrons in the collector. Such a macroscopic amplification of the single electron quantum state resembles the Schrödinger cat paradox. Similarly, it is rather natural to assume that the actual realization of the electron position inside the double-dot takes place before the observer looks on the detector. Yet, it still must be related to the measurement process that detects the occupied dot. However, it is not clear what does constitute the detection in our case. For instance, one can suggest that a penetration of *one* electron to the collector is already the measurement, since it indicates that the left dot is occupied. On the other hand, such a single electron is not actually observed. Thus, one can define a measurement

in an alternative way, as a process that outcome is stored in a stable form, ready to be retrieved by an observer [20]. In this case the right reservoir of the detector must be coupled with an another macroscopic device (the "pointer") that actually counts the accumulated charge. If such a pointer responds only to a macroscopic amount of charge accumulated in the collector, the measurement would be completed much later than in the first case.

A. Continuous collapse

Let us begin with the first scenario. In this case the "measurement time" [16], $t_{ms} = 1/D_1$, is the time of one-electron penetration to the collector when the left dot is occupied. If we assume that each time-interval t_{ms} the system starts its evolution with the new initial conditions, even if the collector charge is not actually counted, we arrive to a continuous collapse model (c.f. [22]). Yet, such an extreme scenario would result in significant violation of the quantum mechanical predictions. Indeed, consider the initial conditions corresponding to the blocked point-contact (the right dot is occupied) and the right reservoir is empty: $\sigma_{22}^{(n)}(0) = \delta_{0n}$ and $\sigma_{11}^{(n)}(0) = \sigma_{12}^{(n)}(0) = 0$ in Eqs. (6). One easily obtains from Eqs. (6) that the probability of finding zero electrons in the collector at $t = t_{ms}$ is $P_0(t_{ms}) \simeq 1 - 2\Omega_0^2 t_{ms}^2$. Then after $D_1 t$ such successive measurements the probability of finding the system undecayed at the time t is

$$P_0(t) = \left(1 - \frac{2\Omega_0^2}{D_1^2}\right)^{D_1 t} + \mathcal{O}\left(\frac{\Omega_0}{D_1}\right)^4 \simeq 1 - \frac{2\Omega_0^2}{D_1} t \tag{21}$$

Therefore the point-contact remains blocked (Zeno time) for the time-interval $D_1/2\Omega_0^2$. On the other hand, the non-interrupted evolution of Eqs. (6) yields four times less value ($D_1/8\Omega_0^2$) for the corresponding Zeno time, Eq. (10). Thus the continues collapse scenario predicts different dwell-time for the observed electron, in a comparison with the Schrödinger evolution. Notice, however, that if we choose the measurement time as corresponding to penetration of four electrons, $t_{ms} = 4/D_1$, the continuous collapse would yield the same average dwell-time, as the Schrödinger evolution (c.f. [21]). Yet, even in this case, the distribution $P_0(t)$ as a function of time would be still different.

In fact, the predictions of the continuous collapse model and the quantum mechanics can be checked experimentally by switch on the pointer at a corresponding time. However, it is quite clear that the continuous collapse means *strong* violation of the quantum mechanics. In order to avoid it, we assert that whenever the "actual fact" is realized, the entire system proceeds its quantum evolution with no interruption for a long (Zeno) time τ_Z, Eq. (10). This time is completely defined by the Schrödinger equation. Yet, the main question still remains: when these mysterious quantum jumps can take a place. We claim here that this problem can also be investigated experimentally. Such a unique possibility is provided by the large Zeno time τ_Z that can reach macroscopic time-scales for $D_1/\Omega_0 \to \infty$.

B. Spontaneous collapse

Consider again the double-dot electron, which is initially in the ground state (symmetric superposition). As we demonstrated above that the Schrödinger evolution of the entire system generates two peaks in the distribution $P_n(t)$, Fig. 5, corresponding to the electron localized in the right or in the left dot. Let us assume that one of these possibilities is always realized on the microscopic time-scale, i.e. for $t \sim 1/D_1$. Then the electron would stay in the same dot for a long time, τ_Z. Afterwards it can be found in the second dot with the probability 1/2. Hence, one can expect that the number of electrons accumulated in the collector, $N(t)$, would display the following behavior, as shown schematically in Fig. 6 by the solid line.

In fact, there is no a-priory time-scale for these jumps. For instance, a localization of the observed electron in one of the dots can happen on the time-scale $t_0 \gg 1/D_1$, when the number of electrons in the collector ($D_1 t_0$) becomes macroscopically large. In order to determine t_0 experimentally we connect the right reservoir with a macroscopic "pointer" that actually counts electrons in the collector, and displays the relevant data directly to the observer. We assume that the pointer starts the counting only after the number of electrons in the collector reaches some threshold value $\bar{N}$, i.e. for $t > \bar{t} = \bar{N}/D_1$. This threshold $\bar{N}$

can be varied by the experimentalist in a wide interval. But we always assume that $\bar{t} < \tau_Z$.

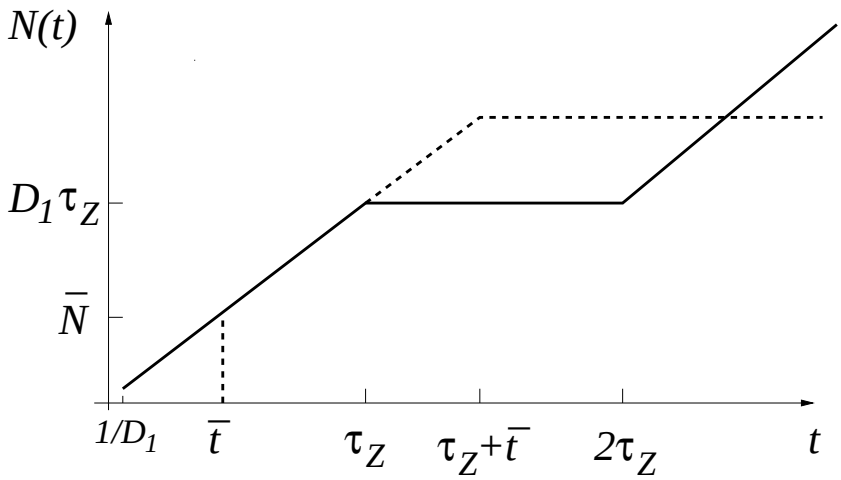

Fig. 6. The number of electron penetrating to the collector as a function of time. The dashed line corresponds to the actual pointer display if the quantum jump happens at $\bar{t} = \bar{N}/D_1$, where $\bar{N}$ is the pointer threshold.

The entire system can be described quantum-mechanically by adding the corresponding terms in the total Hamiltonian, Eq. (2)

$$\mathcal{H} = \mathcal{H}_{PC} + \mathcal{H}_{DD} + \mathcal{H}_P + \mathcal{H}_{int} + \mathcal{H}'_{int}, \tag{22}$$

where $\mathcal{H}_P$ and $\mathcal{H}'_{int}$ describe the pointer and its interaction with electrons in the collector. These terms can be written in a form of the tunneling Hamiltonian, Eqs. (3), where the threshold $\bar{N}$ can be accounted for in $\mathcal{H}'_{int}$ by increasing the number of the corresponding creation and annihilation operators. Note that the pointer does not interact with the double-dot. It is rather clear that such it cannot influence the time-evolution of $P_n(t)$, except for a modification of the decoherence rate $D_1 \to D'_1$. The latter in fact, can be made arbitrary small, $\Delta D_1/D_1 \to 0$.

Let us assume that the pointer threshold time $\bar{t} > t_0$. It implies that the pointer displays the electron localization in the left dot at $t = \bar{t}$, i.e. later than it actually happened. As a result, the electron dwell-time shown by the pointer becomes $\tau_Z + t_0 - \bar{t} < \tau_Z$. Therefore,

by decreasing the pointer threshold $\bar{N}$, the dwell-time shown by the pointer would always increase, unless $\bar{t} < t_0$. It would allow us to determine the time-scale for the spontaneous collapse.

C. Collapse due to observation

The above scenarios of spontaneous collapse assume the existence of parameters that determine the collapse time-scale. However, these parameters cannot be obtained within the Quantum Mechanics. It would imply that the Quantum Mechanics is not a complete theory. On the other hand, no such parameters are needed if we assume that the collapse takes place whenever the relevant information on the system can be directly available to the observer. Although this point of view looks very strange, it is rather close to the von-Neumann and even to the "orthodox" (Copenhagen) interpretation of the measurement in quantum mechanics [1]. Most important, however, that such a scenario has definite experimental consequences in the framework of our setup. Indeed, in this case the collapse should *always* take place whenever the pointer starts to respond to an accumulated charge, i.e. at the time $\bar{t}$. This is because the left dot is *definitely* occupied when the pointer displays the charge. Otherwise, the point-contact is blocked and the collector charge cannot reach its threshold value $\bar{N}$. (The same arguments are applied, when the pointer does not show any collector charge at $t = \bar{t}$). As a result, the pointer would display the same dwell-time τ_Z (the dashed line in Fig. 6) for any values of $\bar{N}$.

Let us demonstrate on a simple example that such a scenario is somehow inherent in the quantum-mechanical approach. Consider the point-contact detector detached from the double-dot. In this case the detector behavior is described by Eq. (11) that gives the probability distribution $p_n(t)$, Eq. (13), of finding n electrons in the collector at time t. Although this equation was obtained from the many-body Schrödinger equation (see Appendix), it can be viewed as the classical probabilistic equation. However, the latter implies that its outcome does depend on the information, obtained by an observer at any intermediate stages

(the Bayes principle). Indeed, let us assume that the detector displays N_1 electrons at some time t_1. Then it is quite clear that the distribution $p_n(t)$ for $t \geq t_1$ is given by the same Eq. (11), but with new initial conditions at $t = t_1$ [23]. One obtains

$$p_n(t) \simeq \frac{1}{\sqrt{2\pi D_1(t-t_1)}} \exp\left[-\frac{(D_1 t - n + \Delta N)^2}{2D_1(t-t_1)}\right], \tag{23}$$

where $\Delta N = N_1 - D_1 t_1$. Comparing this result with Eq. (13) we find that $p_n(t)$ has the same group velocity (the average current), but the width of the distribution is narrower. That means that the information acquired during the measurement, affects the electron probability distribution $p_n(t)$. (Actually, it affects the fluctuation, but not the average value of the observed quantity). Notice that this result is quite natural from the classical point of view. Indeed, the probabilistic description of classical systems is not a complete one. The measurement just improves our knowledge on the system, so the statistical uncertainty diminishes.

As a matter of fact, Eq. (11) has been derived quantum-mechanically, from the many-body Schrödinger equation. Nevertheless, we must obtain the same Eq. (23) for $p_n(t)$, if the number of electrons in the collector is actually known at $t = t_1$. Otherwise, the quantum mechanics does not reproduce its classical limit. It means that whenever the pointer starts to deliver the relevant information to an observer (i.e. at $t_1 = \bar{t}$), the probability distribution should jump from Eq. (13) to Eq. (23). The same should be expected when the detector is coupled with the double-dot. This would imply that the moment of quantum jumps is determined by the pointer sensitivity.

VI. DISCUSSION

It is well-know that the quantum mechanics gives only a *conditional* probability. The same holds for the classical probabilistic description. Therefore an information on the system obtained by a measurement, changes the probabilities of the following events (the wave-function collapse). In the classical case this obviously cannot influence the true system

behavior, providing that system is not distorted by the detector. Indeed, the probabilities in the classical case represent only our ignorance as to the true state.

The situation with the quantum mechanical probabilities is not so clear. The probability amplitudes there must be ascribe some objective meaning independent of human knowledge [24]. For instance, an information on the system true state implies the vanishing of the corresponding off-diagonal density-matrix elements, which can influence the system behavior. Such an effect cannot be totally attributed due to the decoherence, as can be seen in an example of continuous measurement. In this case the apparatus (and also the environment) generates decoherence, which steady diminishes the off-diagonal density matrix elements, but never makes them *zero*. It manifests itself in the quantum Zeno effect which slows down quantum transitions between the isolated states. Nevertheless these transitions, which proceed via the off-diagonal density-matrix elements, are never totally interrupted by the decoherence. The same remains valid by extending the quantum mechanical description via von Neumann hierarchy [1] (a system "measured" by another system etc). In this way one can only increase the decoherence rate. Yet, an "observation" which nullifies the off-diagonal density-matrix elements would not be singled out.

This severe problem of quantum measurement cannot be resolved by using only the theoretical arguments. In this paper we proposed to investigate the wave-function collapse in experiments with continuous monitoring of a single quantum system. Such experiments are now within reach of present technology. The main idea consists in freezing the system in the same state for a very long time (the Zeno time, τ_Z) due to its continuous monitoring. The Zeno time is evaluated by using the Schrödinger equation for the entire system, including the detector, connected with a macroscopic pointer. The latter is switched on automatically at $t = t_0$, where $t_0 < \tau_Z$. (The "switching on" can be made gradually, but on the scale much smaller than τ_Z). Then, if the collapse takes place before the system is observed, the calculated Zeno time would be different from that shown by the pointer. Since t_0 varies with the pointer threshold, it would be possible to single out experimentally the time-scale for the wave-function collapse. This would be extremely important in understanding the

nature of the collapse and whether it is related with the actual information available to the observer.

We have not investigated in this paper all possible consequences of the measurement collapse. For instance, the measurement with weakly responding detector [17], or the influence of AC voltage applied across the point-contact detector [19]. Yet, we believe that our model for continuous measurement of a single system is suitable for investigation of difference sides of the measurement problem and allows their experimental realization. We also expect that this model can be adapted for optical experiments with a single atom [5].

VII. ACKNOWLEDGMENTS

I owe special thanks to E. Buks for attracting my attention to the problem of detector current and numerous fruitful discussions. Special thanks to Y. Aharonov for very useful discussions, which helped me in elaboration of different aspects of the measurement problem. I am also grateful to M. Heiblum, M. Kleber, A. Korotkov, M. Marinov, L. Pitaevskii and D. Sprinzak, for useful discussions.

APPENDIX A: QUANTUM-MECHANICAL DERIVATION OF RATE EQUATIONS FOR A POINT-CONTACT DETECTOR

Here we present the derivation of classical rate equations (11), starting from the Schrödinger equation. By using the same technique we also derive the average current and the current fluctuations and compare our results with those existing in the literature.

Consider the point-contact detector, describing by the tunneling Hamiltonian, $\mathcal{H}_{PC}$, Eq. (3a). The initial (vacuum) state ($|0\rangle$) is the state, where the levels in the emitter and the collector are initially filled up to the Fermi energies μ_L and μ_R respectively, Fig. 1. The many-body wave function for this system can be written in the occupation number representation as

$$|\Psi(t)\rangle = \left[b_0(t) + \sum_{l,r} b_{lr}(t) a_r^\dagger a_l + \sum_{l<l',r<r'} b_{ll'rr'}(t) a_r^\dagger a_{r'}^\dagger a_l a_{l'} + \cdots \right] |0\rangle \ , \tag{A1}$$

where $b(t)$ are the time-dependent probability amplitudes to find the system in the corresponding states with the initial condition $b_0(0) = 1$, and all the other $b(0)$'s being zeros (cf. with Eqs. (4) for the entire system). Substituting it into the Shrödinger equation $i|\dot{\Psi}(t)\rangle = \mathcal{H}_{PC}|\Psi(t)\rangle$ and performing the Laplace transform: $\tilde{b}(E) = \int_0^\infty e^{iEt} b(t) dt$ we obtain an infinite set of the coupled equations for the amplitudes $\tilde{b}(E)$:

$$E\tilde{b}_0(E) - \sum_{l,r} \Omega_{lr} \tilde{b}_{lr}(E) = i \tag{A2a}$$

$$(E + E_l - E_r)\tilde{b}_{lr}(E) - \Omega_{lr}\tilde{b}_0(E) - \sum_{l',r'} \Omega_{l'r'} \tilde{b}_{ll'rr'}(E) = 0 \tag{A2b}$$

$$(E + E_l + E_{l'} - E_r - E_{r'})\tilde{b}_{ll'rr'}(E) - \Omega_{l'r'}\tilde{b}_{lr}(E) + \Omega_{lr}\tilde{b}_{l'r'}(E) - \sum_{l'',r''} \Omega_{l''r''} \tilde{b}_{ll'l''rr'r''}(E) = 0 \tag{A2c}$$

$$\cdots\cdots\cdots\cdots\cdots$$

Eqs. (A2) can be substantially simplified by replacing the amplitude $\tilde{b}$ in the term $\sum \Omega \tilde{b}$ of each of the equations by its expression obtained from the subsequent equation [3,2]. For example, substituting $\tilde{b}_{lr}(E)$ from Eq. (A2b) into Eq. (A2a), one obtains

$$\left[E - \sum_{l,r} \frac{\Omega^2}{E + E_l - E_r} \right] \tilde{b}_0(E) - \sum_{ll',rr'} \frac{\Omega^2}{E + E_l - E_r} \tilde{b}_{ll'rr'}(E) = i, \tag{A3}$$

where we assumed that the hopping amplitudes are weakly dependent functions on the energies $\Omega_{lr} \equiv \Omega(E_l, E_r) = \Omega$. Since the states in the reservoirs are very dense (continuum), one can replace the sums over l and r by integrals, for instance $\sum_{l,r} \ \rightarrow \ \int \rho_L(E_l)\rho_R(E_r)\, dE_l dE_r$, where $\rho_{L,R}$ are the density of states in the emitter and collector. Then the first sum in Eq. (A3) becomes an integral which can be split into a sum of the singular and principal value parts. The singular part yields $i\pi\Omega^2\rho_L\rho_R V_d$, and the principal part is merely included into redefinition of the energy levels. The second sum (non-factorized term) in Eq. (A3) can be neglected in the limit of large bias $V_d \gg \Omega^2\rho$. Indeed, by replacing $\tilde{b}_{ll'rr'}(E) \equiv \tilde{b}(E, E_l, E_{l'}, E_r, E_{r'})$ and the sums by the integrals we find that the integrand has

the poles in $E_{l,r}$-variables on the same sides of the integration contours. It means that the corresponding integral vanishes.

Applying analogous considerations to the other equations of the system (A2), we finally arrive to the following set of equations:

$$(E + iD/2)\tilde{b}_0 = i \tag{A4a}$$

$$(E + E_l - E_r + iD/2)\tilde{b}_{lr} - \Omega\tilde{b}_0 = 0 \tag{A4b}$$

$$(E + E_l + E_{l'} - E_r - E_{r'} + iD/2)\tilde{b}_{ll'rr'} - \Omega\tilde{b}_{lr} + \Omega\tilde{b}_{l'r'} = 0, \tag{A4c}$$

$$\cdots\cdots\cdots\cdots\cdots$$

where $D = 2\pi\Omega^2\rho_L\rho_R V_d$.

The amplitudes $\tilde{b}$ are directly related with the corresponding probabilities, $p_n(t)$, of finding n electrons in the collector:

$$p_0(t) = |b_0(t)|^2, \quad p_1(t) = \sum_{l,r} |b_{lr}(t)|^2, \quad p_2(t) = \sum_{ll',rr'} |b_{ll'rr'}(t)|^2, \ \cdots \ . \tag{A5}$$

By applying the inverse Laplace transform

$$p_n(t) = \sum_{l\ldots,r\ldots} \int \frac{dEdE'}{4\pi^2} \tilde{b}_{l\cdots r\cdots}(E)\tilde{b}^*_{l\cdots r\cdots}(E')e^{i(E'-E)t} \, . \tag{A6}$$

one can transform Eqs. (A4) into the rate equations for $p_n(t)$ (c.f. [3,2]). We find

$$\dot{p}_0(t) = -Dp_0(t) \tag{A7a}$$

$$\dot{p}_1(t) = Dp_0(t) - Dp_1(t) \tag{A7b}$$

$$\dot{p}_2(t) = Dp_1(t) - Dp_2(t) \tag{A7c}$$

$$\cdots\cdots\cdots\cdots\cdots$$

which are the classical rate equations (11).

The essential point in our quantum-mechanical derivation of Eqs. (A7) is neglect of the "cross" terms, namely those where the amplitudes $\tilde{b}$ cannot be factorized out (like the second term in Eq. (A3)). As a result we obtain Eqs. (A4), which lead eventually to the

rate equations (A7). Although the neglect of the cross-terms can be justified in the limit of $V_d \gg \Omega^2\rho$, we nevertheless expect that Eqs. (A4) are valid even beyond that limit. For instance, we demonstrate below, that these equations result in correct expressions for the average current and the current fluctuations.

1. Average current

The current operator is defined as a commutator of the accumulated charge with the Hamiltonian

$$\hat{I} = ie\left[\mathcal{H}_{PC}, \sum_r a_r^\dagger a_r\right] = ie\sum_{l,r}\Omega_{lr}(a_l^\dagger a_r - a_r^\dagger a_l) \tag{A8}$$

Using Eqs. (A1), (A8) we find the following expression for the average current

$$I(t) = \langle\Psi(t)|\hat{I}|\Psi(t)\rangle = 2e\ \mathrm{Im}\left[\sum_{l,r}\Omega_{lr}\ b_0(t)b_{lr}^*(t) + \sum_{ll'rr'}\Omega_{l'r'}\ b_{lr}(t)b_{ll'rr'}^*(t) + \cdots\right] \tag{A9}$$

As in the previous consideration we replace the sums by the integrals. By applying the inverse Laplace transform and using Eqs. (A4) we can carry out all the integrations analytically. For instance,

$$\sum_{l,r}\Omega_{lr}b_{lr}^*(t) = \int\frac{dE}{2\pi}e^{iEt}\int\frac{\rho_L\rho_R\Omega^2\ \tilde{b}_0^*(E)}{E+E_L-E_R}dE_L dE_R = i\pi\rho_L\rho_R eV_d\ \Omega^2\ b_0^*(t) \tag{A10}$$

The same procedure can be applied for other terms in Eq. (A9). Finally, by taken into account the normalization condition of the wave function, $\langle\Psi(t)|\Psi(t)\rangle = 1$, one finds

$$I(t) = 2e^2\pi\rho_L\rho_R\Omega^2 V_d\left[|b_0(t)|^2 + \sum_{l,r}|b_{lr}(t)|^2 + \cdots\right] = 2e^2\pi\rho_L\rho_R\Omega^2 V_d\,. \tag{A11}$$

By using $(2\pi)^2\Omega^2\rho_L\rho_R = T$ [13], where T is the transmission probability, we can rewrite the current as $I = e^2 T\, V_d/(2\pi)$. This coincides with the well known Landauer formula [12].

2. Current fluctuations

Let us evaluate the average of $\hat{I}^2$ operator. Using Eq. (A8) one can write

$$\langle\Psi(t)|\hat{I}^2|\Psi(t)\rangle = -e^2\langle\Psi(t)|\sum_{lr,l'r'}\Omega_{lr}\Omega_{l'r'}(a_l^\dagger a_r - a_r^\dagger a_l)(a_{l'}^\dagger a_{r'} - a_{r'}^\dagger a_{l'})|\Psi(t)\rangle\,. \tag{A12}$$

Now we split this sum into two parts corresponding to $lr \neq l'r'$ and $lr = l'r'$. Then, using Eq. (A1) we rewrite Eq. (A12) as

$$\langle\Psi(t)|\hat{I}^2|\Psi(t)\rangle = 4e^2\ \mathrm{Re}\left[\sum_{lr,l'r'}\Omega_{lr}\Omega_{l'r'}b_0(t)b^*_{ll'rr'}(t) + \cdots\right] + 2e^2\sum_{lr}\Omega_{lr}^2\,. \tag{A13}$$

The second term can be written as $2e\Delta\nu I$, where $\Delta\nu$ is the band width and I is the average current, Eq. (A11). This expression corresponds to Shottky noise. Consider now the first sum in Eq. (A13). It can be evaluated in the same way as Eq. (A9). Indeed, by replacing the sum by the integral and using the inverse Laplace transform and Eqs. (A4) we obtain

$$\sum_{lr,l'r'}\Omega_{lr}\Omega_{l'r'}b^*_{ll'rr'}(t) = \int\frac{dE}{2\pi}e^{iEt}\int\frac{\rho_L^2\rho_R^2\Omega^4\ \tilde{b}_0^*(E)dE_LdE_L'dE_RdE_R'}{(E+E_L+E_L'-E_R-E_R')(E+E_L-E_R)} \tag{A14}$$

Taking into account the contributions from the poles and the normalization of the wave function we find that the first term of Eq. (A13) can be represented as $-e^3\ T^2V_d\Delta\nu/2\pi$. Finally the average current fluctuation can be written as

$$\langle(\Delta I)^2\rangle = 2e\ \Delta\nu\frac{e^2V_d}{2\pi}T(1-T)\,. \tag{A15}$$

This coincides with the result obtained earlier by using different techniques [25].

REFERENCES

[1] J. von Neumann, *Mathematische Grundlagen der Quantentheorie* (Springer, Berlin, 1931).

[2] S.A. Gurvitz and Ya.S. Prager, Phys. Rev. B**53**; 15932 (1996); S.A. Gurvitz, Phys. Rev. **B57**, 6602, (1998).

[3] S.A. Gurvitz, Phys. Rev. B**56**, 15215 (1997).

[4] W.H. Zurek, Physics Today **44**, No. 10, 36 (1991); *ibid*, **46**, No. 4, 13 (1993).

[5] A. Beige and G.C. Hegerfeldt, J. Phys. A**30**, 1323, (1997); M.B. Plenio and P.L. Knight, Rev. of Mod. Phys. **70**, 1998, (1998).

[6] S.A. Gurvitz, in *Proceedings of the V. Workshop on Nonequilibrium Physics at Short - Time Scales*, Rostock, April 27-30, 1998; quant-ph/9806050.

[7] A. Shnirman and G. Schön, and Z. Hermon, Phys. Rev. Lett. **79**, 2371 (1997); D.V. Averin, cond-mat/9706026.

[8] This might be considered as the central problem of measurement theory, see P.W. Anderson, in *The Lesson of Quantum Theory*, (Elsevier Science Publishers B.V., 1986), p. 23.

[9] Y. Imry, cond-mat/9807306.

[10] M. Field *et al.*, Phys. Rev. Lett. **70**, 1311 (1993).

[11] A similar nondistracting continuous monitoring of electrons in the linear superposition has been realized in a recent elegant experiment, E. Buks, R. Shuster, M. Heiblum, D. Mahalu and V. Umansky, Nature **391**(1), 871 (1998).

[12] R. Landauer, IBM J. Res. Dev. **1**, 223 (1957); R. Landauer, J. Phys. Condens. Matter **1**, 8099 (1989).

[13] J. Bardeen, Phys. Rev. Lett. **6**, 57 (1961).

[14] L.S. Levitov, H. Lee, and G.B. Lesovik, J. Math. Phys. **37**, 4845 (1996).

[15] B. Misra and E.C.G. Sudarshan, J. Math. Phys. **18**, 756 (1977); R.A. Harris and L. Stodolsky, Phys. Lett. B**116**, 464 (1982); E. Block and P.R. Berman, Phys. Rev. A**44**, 1466 (1991); V. Frerichs and A. Schenzle, Phys. Rev. A**44**, 1962 (1991); C. Presilla, R. Onofrio and U. Tambini, Ann. of Phys. **248**, 95 (1996), and references therein.

[16] A. Shnirman and G. Schön, Phys. Rev. B**57**, 15400 (1998).

[17] A.N. Korotkov, quant-ph/9807051.

[18] L. Stodolsky, quant-ph/9805081.

[19] G. Hackenbroich, B. Rosenow, and H.A. Weidenmüller, Phys. Rev. Lett. **81**, 5896 (1998).

[20] D. Home and R. Chattopadhyaya, Phys. Rev. Lett. **76**, 2836 (1996).

[21] L.S. Schulman, Phys. Rev. A**57**, 1509 (1998).

[22] P. Pearle, Phys. Rev. A**39**, 2277 (1989); G.C. Ghirardi, P. Pearle and A. Rimini, Rev. A**42**, 78 (1990).

[23] M. Ozawa, quant-ph/9802022.

[24] E.T. Jaynes, Phys. Rev. **108**, 171 (1957).

[25] M. Büttiker, J. Math. Phys. **37**, 4793 (1996), and references therein.